Photoluminescence properties and excited state dynamics of monolayer perylene on graphite (0001)

Takashi Yamada*

Department of Chemistry, Graduate School of Science, Osaka University, Toyonaka 560-0043, Japan

(Received 17 April 2023; revised 4 September 2023; accepted 30 October 2023; published 22 November 2023)

The correlation between the photoluminescence properties and excited state dynamics of perylene ($C_{20}H_{12}$) formed on a graphite (0001) substrate was investigated at the monolayer limit. Time-resolved two-photon photoemission spectroscopy was used to evaluate the lifetime of the excited state on the order of nanoseconds. On the molecular monolayer films, this unexpectedly long lifetime at the interface is significantly different from those typically observed for adsorption-induced electronic states, where ultrafast decays on the order of femtoseconds are dominant with electron/hole scattering. On the graphite (0001) surface, the standing molecular orientation of perylene indicates that the excited states are electronically decoupled from the substrate, which results in the suppression of the ultrafast nonradiative decay. As a result, orange light luminescence (610 nm) is observed with visible strength, which is ascribed to the deexcitation from the excited state of the dimeric molecular arrangement at the interface. Understanding the photoluminescence properties at the organic/electrode interface could be a key to the realization of organic optoelectronic thin-film devices with only a few molecular layers.

DOI: 10.1103/PhysRevB.108.205422

I. INTRODUCTION

Organic semiconductors have been widely utilized in recent decades for optoelectronic devices such as photodetectors, light-emitting diodes, and solar cells [1,2]. Despite a wide range of applications, elucidation of the physical principles that control the optical excitation/deexcitation processes at the organic/electrode interface remains a subject of intense research. In particular, an understanding of the optoelectronic properties at the organic/substrate interface is indispensable to realize ultrathin organic electroluminescence devices with a few molecular layer thicknesses [3,4]. However, experimental investigation of the photoluminescence (PL) properties has been limited and thus not thoroughly investigated to date, because the excited electrons, holes, and their pairs, i.e., excitons at the interface, are quickly quenched on the order of femtoseconds before light emission. Electron-hole pair recombination (exciton quenching) is enhanced due to the close contact with the substrate that acts as an efficient decay route. Here, the hybridization of the molecular orbital with the electronic states of the substrate plays a crucial role in the ultrafast decay of the excited state [5–8].

In this context, we envisage interface design strategies to suppress the nonradiative decay affected by the substrate. As an appropriate choice of a highly fluorescent molecule, perylene ($C_{20}H_{12}$) [9–15] is adopted as a model molecule [see the inset of Fig. 1(a) for the molecular structure]. Perylene has been an essential organic molecule that is used as a basic structural unit for the production of various derivatives for organic device materials [1,2]. For example, the perylene unit can be incorporated with designed cofacial arrangements as a chromophore [16,17]; this molecule exhibits PL that is characteristic of the excited state of the dimer, i.e., excimer.

The growth of perylene on various substrates has been investigated in the past to investigate molecules that directly contact electrode surfaces [18–23]. On a metallic substrate, the perylene molecule typically adopts flat-lying adsorption with its molecular plane parallel to the substrate, which reflects the effectiveness of its substrate-molecule interaction [18–23]. In this study, a graphite substrate was adopted, where the substrate-molecule interaction is generally considered to be weaker than that of metal substrates. At low temperatures around 80 K, a film with a thickness of one monolayer (1 ML) on a graphite substrate was identified with a long-range ordered structure [24]. Scanning tunneling microscopy (STM) was used to confirm the standing molecular orientation with its short molecular axis parallel to the substrate (see Supplemental Material, Fig. S1 [25]; see also [26–31]). A face to face molecular arrangement composed of the dimer is preferred on a graphite substrate, which indicates that the intermolecular interaction dominates over the substrate-molecule interaction. Therefore, the perylene/graphite interface can be a model system to observe PL in a well-defined environment without the complexity of actual devices.

In this study, the time-dependent excited state dynamics at the perylene/graphite interface was tracked from a femtosecond timescale using two-photon photoemission (2PPE) spectroscopy [32–36]. The formation of the excited state is responsible for the visible light emission, and time-resolved 2PPE (TR2PPE) revealed an extremely long lifetime close to the order of nanoseconds. This exceptionally long lifetime of the excited state at the interface is unusual compared to those observed for adsorption-induced states, such as those derived from the lowest unoccupied molecular orbital (LUMO) and unoccupied surface states. In the case of the monolayer

*tyamada@chem.sci.osaka-u.ac.jp

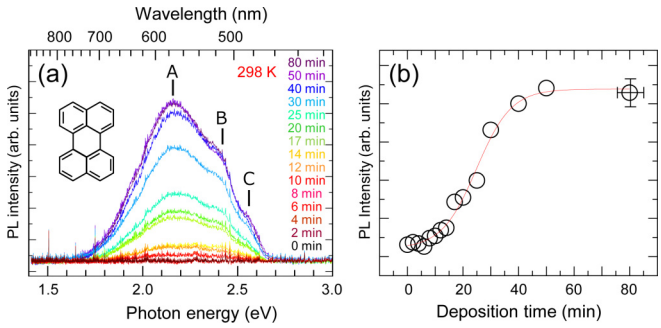

FIG. 1. (a) Photoluminescence (PL) spectra of perylene on single-crystalline graphite as a function of deposition time. Perylene films were excited by a UV light at a photon energy of 4.70 eV (263 nm). The substrate was kept at room temperature (298 K) during the deposition and measurements. The inset shows the molecular structure of perylene. (b) Deposition time dependent PL area intensities integrated from the energy window between 1.6 and 2.7 eV. The sigmoid function (red curve) is overplayed to guide the eye.

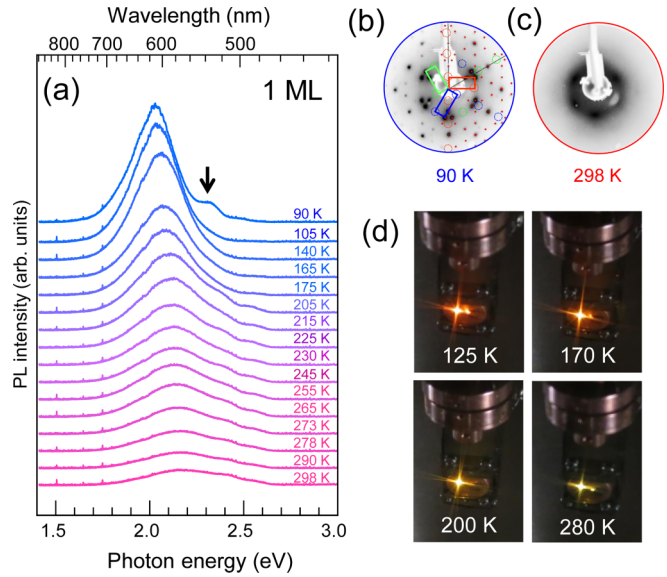

FIG. 2. (a)Temperature-dependent PL spectra for a 1 ML perylene film. As the temperature increases, the peak at around 2.0 eV is weakened and broadened toward the higher-energy side. The black arrow indicates the spectroscopic feature known as the Y (yellow) emission. (b) Contrast-enhanced LEED pattern for a 1 ML perylene film acquired at 90 K. The primary energy of the electron beam (E_p) was 37.0 eV. The reciprocal unit cells along with the three crystallographic directions are shown and some simulated spots are highlighted with red points. Circles indicate absent diffraction spots due to the glide plane symmetry. Black lines indicate the directions of one of the reciprocal lattice vectors of the substrate. (c) LEED pattern of a 1 ML perylene film acquired at 298 K and $E_p = 36.9$ eV. Less-ordered molecular distribution was observed, as characterized by the disk-shaped background with diffuse spots. (d) Photographs taken during the temperature-dependent PL measurements. As the temperature increased, a change in the PL color was observed from orange to yellow-green.

crystalline film investigated here, the formation of the excited state with a long lifetime is responsible for PL, by suppressing nonradiative decay to the substrate.

II. EXPERIMENTAL METHODS

All experiments were conducted under ultrahigh-vacuum (UHV) conditions with a base pressure of less than 1×10^{-10} Torr. Two independent UHV systems were used; one is designed for TR2PPE spectroscopy [37] and the other is for PL spectroscopy and low-energy electron diffraction (LEED) measurements [24]. Two-photon photoemission experiments can also be conducted in the latter PL/LEED chamber. Therefore, the film thickness and homogeneity of monolayer films formed in each UHV system can be cross-checked by monitoring the 2PPE spectra. In 2PPE, an image potential state (IPS) can be detected on the graphite substrate as well as on uniform monolayer films [38]. IPS is an unoccupied surface state; therefore, IPS can be utilized as a sensitive probe to determine the coverage. After completion of the monolayer film in layer by layer growth mode, the IPS on the substrate (IPS_{HOPG}) disappears, and instead, the IPS on the monolayer film ($IPS_{perylene}$) appears [24,37]. (See also Fig. 3.) The maximum coverage of perylene on the room-temperature substrate is restricted to 1 ML, and multilayer growth was not detected [24,37].

The experimental details of the PL spectroscopy measurements have been reported previously [24]. Briefly, perylene films were excited by a UV light at a photon energy of 4.70 eV (263 nm). The UV light was generated by frequency tripling the output of a titanium sapphire laser (MaiTai, Spectra-Physics) operated at a repetition rate of 80 MHz and with a pulse width of 110 fs. The *p*-polarized light was focused on the sample surface with a concave mirror and the power of the laser light was set to less than 0.13 nJ/pulse to avoid degradation of the films.

One-color 2PPE measurements were conducted; i.e., the pump and probe lights were identical. UV light with photon energies from 4.16 to 4.77 eV was employed and the light was shared with that used for the PL spectroscopy. Photoelectrons were detected with an angle-resolved hemispherical energy analyzer (R3000, VG-Scienta) and the overall energy resolution, including the bandwidth of the laser light, was typically less than 30 meV [37,38].

Two types of graphite were employed as substrates. Highly oriented pyrolytic graphite (HOPG; Panasonic) was used for 2PPE. Single-crystalline graphite (SCG; a naturally occurring material purchased from Naturally Graphite) was used for LEED measurements because high crystallinity is essential for diffraction measurements. The substrates were cleaved in air and heated at 670 K for more than 60 h under UHV to ensure outgassing from the interlayer spacing. The superstructure of perylene showed no difference on the HOPG and SCG substrates [37,38]. The spectroscopic features in the 2PPE and PL measurements also showed no difference for either substrate.

Commercially available perylene reagent (> 98%, Tokyo Chemical Industry Co. Ltd.) was purified by three cycles of sublimation under high vacuum ($< 10^{-6}$ Torr) prior to the measurements. Perylene was deposited onto the room-temperature (298 K) substrate from a quartz crucible heated at

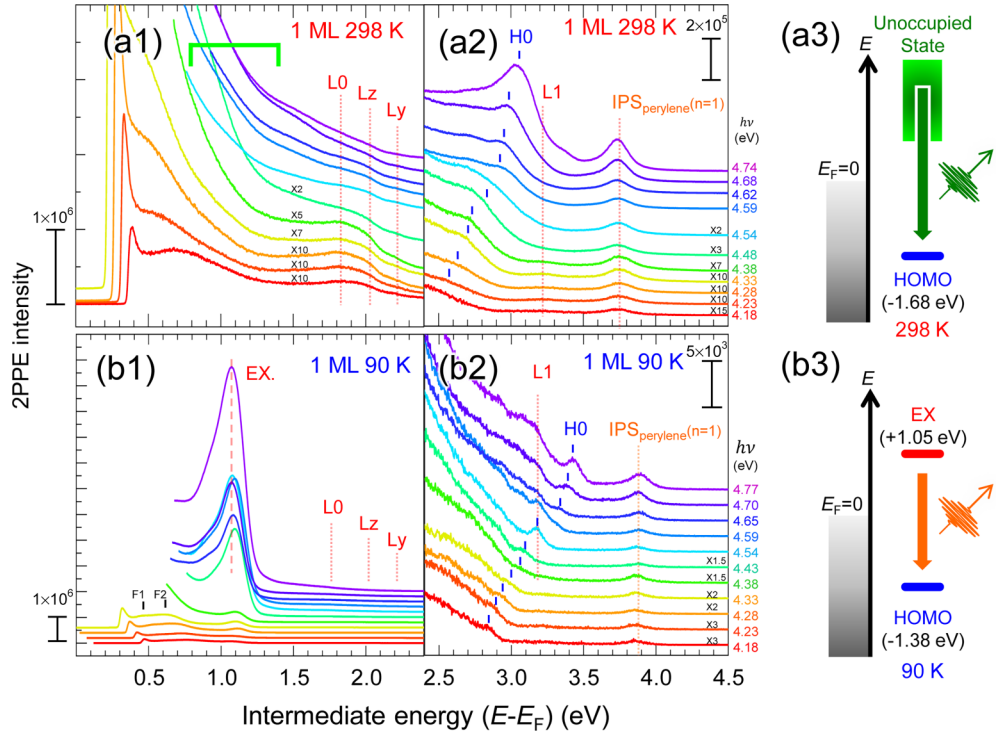

FIG. 3. Photon energy dependent 2PPE spectra of 1 ML perylene films on HOPG acquired at room temperature [(a1,a2), at 298 K] and low temperature [(b1,b2), at 90 K]. The vertical dotted lines are shown to highlight the peaks derived from unoccupied states. The traces in the right-hand panels are expanded by factors of 3 (298 K) and 300 (90 K) relative to those in the left-hand panel. H0 indicates the peak derived from the HOMO. L0 and L1 indicate the peaks derived from LUMO and the next LUMO (LUMO + 1), respectively. Ly and Lz are other unoccupied molecular orbitals. $IPS_{perylene}$ ($n = 1$) indicates the first ($n = 1$) image potential states on the 1 ML perylene film. EX indicates the peak derived from the excited states of dimers. It should be noted that the EX peak was observable at (b1) low temperature but not at (a1) room temperature. F1 and F2 indicate the final states, i.e., unoccupied states above the vacuum level. (a3,b3) represent schematic energy diagrams of PL at 298 and 90 K, respectively.

373 K, while maintaining a background pressure of 1×10^{-8} Torr.

III. RESULTS AND DISCUSSION

A. Coverage-dependent PL spectroscopy

Figure 1(a) shows deposition time dependent PL spectra of perylene on graphite. The substrate was kept at room temperature (298 K) during the deposition and measurements. As the deposition time increased, the intensities of the spectroscopic features *A* (2.15 eV), *B* (2.40 eV), and *C* (2.55 eV) increased. Perylene crystals are known to adopt two polymorphs, i.e., dimeric α-crystal and monomeric β-crystal, and the PL spectra of each polymorph have been reported [9–11]. The PL spectral features in Fig. 1(a) are different from those of crystals; the peak position of *A* was shifted from that of an α-crystal and the spectroscopic feature of peak *B* was less prominent than that of a β-crystal. Therefore, the film possesses a structure different from α- or β-crystals, which is consistent with the room-temperature LEED pattern of the 1 ML film shown in Fig. 2(c), where less-ordered molecular distribution was observed as characterized by the disk-shaped background with diffuse spots.

Figure 1(b) summarizes the PL area intensities in Fig. 1(a) integrated over the energy region between 1.6 and 2.7 eV. The PL intensities were almost saturated over 50 min deposition. In previous studies [24,38–40], it was reported that the maximum perylene coverage on a room-temperature substrate was 1 ML, and subsequent molecular layers could not be grown in UHV (see also Supplemental Material, Fig. S2 [25]). The saturation of the PL intensity in Fig. 1 is consistent with the maximum coverage of 1 ML, as already reported in this system [24,37].

B. Temperature-dependent PL spectroscopy

Depending on the substrate temperature, the PL spectra varied with the change in the film structure. Figure 2(a) shows temperature-dependent PL spectra for a 1 ML perylene film. At 90 K, visible light PL with a wavelength of approximately 610 nm was observed. At low temperatures, a superstructure with long-range order was formed, as shown in the LEED pattern in Fig. 2(b) (see Supplemental Material, Fig. S1 [25]). Previous STM study [24] indicates that the superstructure consists of perylene with a standing molecular configuration and a paired molecular (dimer) arrangement. Therefore, the PL with a wavelength of approximately 610 nm can be ascribed to the PL from the excited state of the dimer, i.e., excimer.

The topmost PL spectrum in Fig. 2(a) was acquired at 90 K; a weak shoulder was observed, as indicated by the

black downward arrow, which corresponds to the so-called yellow (Y) emission. In α-perylene crystals, it was reported that the Y emission is significantly enhanced at temperatures lower than 90 K [9,41–43]. The origin of the Y emission is a metastable excimer, derived from the two next-nearest parallel molecules [43]. The observation of Y emission on the film on the graphite substrate is reasonable because molecules are arranged in a dimeric form similar to the case of an α-crystal. At low temperatures around 105–140 K, the overall PL spectral features are close to those reported for α-crystals [9–11]. A small difference at the peak top in the PL spectra is recognized between the perylene α-crystals [9–11] and monolayer film at 90 K, on the order of less than 0.1 eV. We speculate that the deviation is derived from the difference in the morphology between the film and crystal, i.e., the packing density and/or orientation of molecules.

Figure 2(d) shows a series of photographs taken during the temperature-dependent PL measurement. The PL from monolayer film was observed not only with the spectrometer but also directly with visible strength. As the substrate temperature increased, the color of the PL changed from orange to yellow-green, which is consistent with the changes in the PL spectra in Fig 2(a), where the strong PL spectra at low temperatures shifted and broadened toward the higher-energy side. From a structural point of view, the temperature-dependent quenching of the PL peak at 610 nm in Fig. 2(a) is related to the loss of the dimer structure, as characterized by the temperature-dependent LEED patterns in Figs. 2(b) and 2(c). As in the LEED, STM, and 2PPE results reported previously [24,37], the changes in the PL spectra in Fig. 2(a) were reversible with respect to the substrate temperature.

When we assume that the lifetime of the photoluminescence event is on the order of nanoseconds as reported in the case of dimeric α-crystal [12,13], the spectral width of the PL peak should be less than 1 meV, by considering the uncertainty principle that holds between time and energy. In the cases of single molecules adsorbed on the surface [44] or molecules in liquids [45], PL features with very narrow linewidth were reported. However, Fig. 2 shows that the full width at the half maximum (FWHM) of the PL peak is larger than 0.5 eV, and this value is comparable to that observed for the perylene crystals [9–11]. Here, it should be noted that the monolayer film measured in this study is different from the molecules free from intermolecular interaction. Different from the case of single molecules, the electronic states of molecular films are not discrete but broadened by the energy band formation, thus resulting in the broadening of the PL spectra.

C. Energy level landscape related to PL

Spectroscopic measurements will provide evidence to evaluate the energy level diagram with visible light emission at the perylene/graphite interface. In this context, 2PPE can be a powerful technique with the ability to investigate both occupied and unoccupied states in the vicinity of the Fermi level (E_F) [32–36]. Figure 3 shows 2PPE spectra of a 1 ML perylene film acquired at 298 K [Figs. 3(a1) and 3(a2)] and 90 K [Figs. 3(b1) and (b2)] (see also Supplemental Material, Fig. S3 [25] for logarithmic scale representation of Fig. 3(b1)). The spectra acquired with different photon energies are placed on an intermediate energy scale defined as E_k–$h\nu$, where E_k indicates the kinetic energy of a photoelectron with respect to the E_F and $h\nu$ indicates the photon energy. The peak assignments are based on the procedure reported for sub-ML films [37] and the detailed procedures of the peak assignments are summarized in the Supplemental Material, Fig. S4 [25]. Briefly, the highest occupied molecular orbital (HOMO, H0), LUMO (L0), the second lowest LUMO (L1), and the first member of the image potential states [$IPS_{perylene}(n = 1)$] were assigned close to the energy position reported for sub-ML films [37]. F1 and F2 in Fig. 3(b1) were assigned as the unoccupied state above the vacuum level. For the other unoccupied Lz and Ly features, DFT calculations for a free molecule [37] did not predict the corresponding levels between the L0 and L1; therefore, the origin of the Lz and Ly are left unassigned in the current stage.

Upon lowering the substrate temperature, as shown in Figs. 3(b1) and 3(b2), energy shifts in the peak positions were observed for the unoccupied states [L0, Ly, L1, $IPS_{perylene}$ ($n = 1$), up to 0.1 eV] and the occupied state (H0, ca. 0.3 eV). The most striking difference is the appearance of the intense unoccupied EX peak at low temperatures. The EX peak was observed synchronously with the appearance of orange light emission centered at around 610 nm. At low temperatures, the lowest unoccupied level L0 at $E_F + 1.75$ eV was assigned; however, the EX peak appeared at $E_F + 1.05$ eV, lower than the L0 level. We consider that the deexcitation of the EX state corresponds to the PL from the excimer, as schematically shown in Fig. 3(b3).

In the 2PPE experiments conducted at low temperatures, the energy difference between HOMO and LUMO is 3.1 eV (judged from the peak top energy position; see Supplemental Material, Fig. S5 [25]), and the corresponding photoluminescence photon energy is centered at 2.0 eV [see Fig. 2(a)]. In the case of the dimeric α-crystal, the HOMO-LUMO transition is assigned at 2.98 eV [13] and photoluminescence photon energy is reported to be 2.1 eV [9,13]. By taking the exciton binding energy to be about 0.9–1.1 eV, the energy difference between the HOMO-LUMO gap and photoluminescence photon energy is roughly in agreement for crystals and monolayer film reported in this study. In 2PPE, the energy difference between HOMO-EX (2.4 eV) and the photoluminescence photon energy is 0.4 eV. We have performed experiments with some experimental runs and confirmed that this difference is not an artifact but intrinsic. In our experimental setup, we observed photoemission at around the $\bar{\Gamma}$ point at the surface Brillouin zone. In the case of crystals, the band structure of the HOMO and LUMO is not flat but dependent on the wave vector [13]. Therefore, specific band structures may contribute to the energy difference between HOMO-EX (2.4 eV) and the photoluminescence photon energy (2.0 eV); the optical band gap different from that evaluated at the $\bar{\Gamma}$ point may contribute to the energy difference.

As the substrate temperature increased, the intense EX peak lost its intensity and broadened with the tail component toward the higher-energy side, as shown in Fig. 3(a1). In addition, the HOMO level shifted ca. -0.3 eV, which is also summarized in the Supplemental Material, Fig. S5 [25]. The temperature-dependent 2PPE behavior is linked to the change in the PL spectra. In Fig. 2(a), the PL spectra were broadened

and the overall PL intensity decreased with an increase in the substrate temperature. As schematically shown in Figs. 3(a3) and 3(b3), the synergistic effect of the EX peak broadening and the energy shift of the HOMO toward higher binding energy contribute to the widening of the gap between the HOMO and EX, which leads to the higher photon energy emission at around room temperature. Using temperature-dependent 2PPE and PL spectroscopy, the deexcitation process via photon emission can thus be interpreted for organic films with a single monolayer thickness.

D. Correlation between PL properties and excited state dynamics

The 2PPE technique is based on pump-probe spectroscopy using ultrafast pulses [32–37]. Therefore, the time-dependent behaviors of excited electrons with photoholes, the formation of electron-hole pairs (excitons), and charge transport properties can be tracked from the femtosecond timescale. By focusing on the 1 ML perylene films at low temperatures, as shown in Figs. 3(b1) and 3(b2), the excited state dynamics is tracked and the correlation with the PL properties can be discussed. Time-resolved experiments at room temperature were difficult because the film was less ordered [see Fig. 2(c)] and the one-photon photoemission peak overlapped with unoccupied states that are responsible for PL.

Figure 4(a) shows a series of time-resolved 2PPE spectra for a 1 ML perylene film acquired at 90 K. To track the time-dependent event of 2PPE peaks assigned in Fig. 3, the photon energy was set at 4.77 eV for off-resonant conditions. In Fig. 4(a), the spectrum acquired at a 100 ps delay time was subtracted from the raw 2PPE spectrum (see Supplemental Material, Fig. S6 for raw TR2PPE spectra [25]). Time traces of the peak intensities for L0, L1, and $\mathrm{IPS}_{\mathrm{perylene}}$ $(n = 1)$ are shown in Figs. 4(b)–4(d), respectively. A pulse width of 110 fs was used for quantitative analysis of the time traces. This value was determined from time traces of autocorrelation measured on a clean HOPG substrate at a photoelectron energy of $E_{\mathrm{F}} + 2.0$ eV. This energy corresponds to the position just above the unoccupied π^* band and the lifetime of the excited electron was reported to be less than 20 fs [46,47], which is shorter than the pulse width determined in this study. This pulse width was tentatively adapted without further pulse compression to maintain the energy resolution of the 2PPE spectra.

In Figs. 4(b)–4(d), the fitted curves (red) were convoluted using the autocorrelation of the laser pulse (black) and the lifetime of the corresponding components (blue). The lifetimes in Figs. 4(b)–4(d) were evaluated on the order of 50–60 fs, which corresponds to almost half of the pulse width. In the case of the first member of IPS [IPS $(n = 1)$] observed on the monolayers of phthalocyanines and polyaromatic hydrocarbons, the reported lifetimes typically range from 20 to 40 fs [48,49]. Therefore, the lifetime of the IPS $(n = 1)$ observed in this study (62.2 fs) is considered to be the minimum lifetime that can be evaluated in the current experimental setup.

On the other adsorption-induced states of L0 and L1 shown in Figs. 4(b) and 4(c), the lifetimes were on the order of 50–60 fs. The observed ultrafast lifetimes indicate that excited charges are short lived and decay mainly via a nonradiative

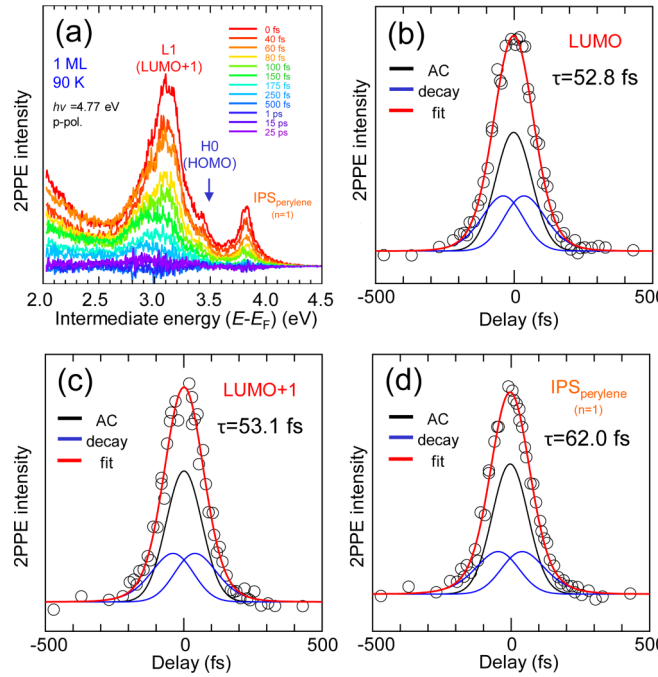

FIG. 4. (a) Time-resolved 2PPE spectra for a 1 ML perylene film acquired at 90 K and at a photon energy of 4.77 eV. The spectrum acquired at 100 ps delay time was subtracted from the raw 2PPE spectrum. (b–d) Pump-probe delay time dependence of intensities for (b) LUMO, (c) LUMO + 1, and (d) $\mathrm{IPS}_{\mathrm{perylene}}$ $(n = 1)$. The pulse width of the laser light was 110 fs, determined on a clean graphite substrate. In (b–d), open circles indicate experimental data points. Black, blue, and red lines indicate the components of autocorrelation (AC) of the pump-probe pulses, exponential decay, and the summation of these two components (black and blue lines), respectively. For (b–d), the estimated lifetimes were on the order of 50–60 fs, close to the detection limit in the current experimental setup.

pathway to the substrate. As a possible scenario for the ultrafast decay in Figs. 4(b) and 4(c), the charge transfer across the molecule/substrate interface can be considered. For example, in the case of the LUMO-derived level of a rubrene monolayer film on HOPG [50], the hybridization of the film and substrate wave functions were reported. As a result, holes exist partly in the substrate and are quickly screened after excitation. In this system with perylene on graphite, although the interaction between the molecule and substrate is moderate due to the standing molecular orientation, electrons in the LUMO and LUMO + 1 can be quenched within an ultrafast timescale. The hole in the HOMO-derived level will also be quickly filled by the electron in the substrate, due to hybridization of the molecular orbital with that of the substrate. As another competitive pathway for quenching, the energy transfer process, i.e., the excitation transfer via Coulombic field coupling, should also be examined [51,52]. Perylene/graphite has a maximum coverage of 1 ML, so that coverage-dependent measurements are not possible; therefore, we cannot distinguish whether the energy transfer to the substrate is a primary decay process or not. Here we could conclude that the ultrafast decay to a sea of electrons on the substrate occurs in the case of the adsorption-induced states as shown in Figs. 4(b) and 4(c).

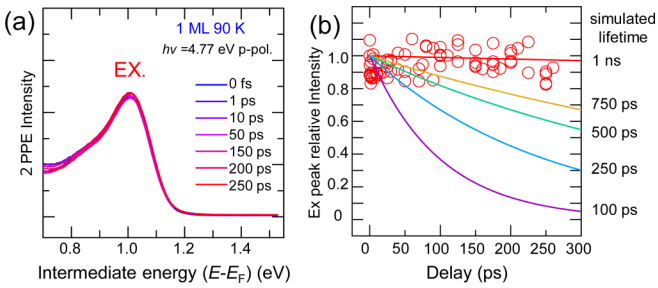

FIG. 5. (a) Time-resolved 2PPE spectra of the EX peak for a 1 ML perylene film. The spectra were acquired at 90 K using a photon energy of 4.77 eV. (b) Delay time dependent intensities of the EX peak (red open circles) and estimated changes of EX peak intensities with specific lifetimes (exponential decay curves shown with solid lines). Unlike the time-resolved traces shown in Fig. 4, the intensities are almost constant with the small fluctuation of the data, which indicates the formation of an apparent steady state within the measured timescale.

Next, we focus on the EX peak observed at low temperatures, for which the visible light emission is responsible. Figure 5(a) shows time-resolved 2PPE spectra of the EX peak for a 1 ML perylene film at 90 K. The spectral features are almost unchanged, irrespective of the delay time, and this behavior is completely different from that observed for adsorption-induced states discussed in Fig. 4. Figure 5(b) shows delay time dependent intensities of the EX peak. The EX peak intensities fluctuate within the experimental error but are almost constant within the maximum pump-probe delay of 250 ps in the current experimental setup. From Fig. 5(b), it seems as if a steady state is formed with a quite long lifetime; the spectral features did not change and showed no tendency to decrease in intensity and peak shift. In Fig. 5(b), changes in EX peak intensities are simulated with specific lifetimes, and the lifetime of the EX state is estimated to be at least on the order of nanoseconds. Full lifetime tracking at the nanosecond scale is outside the range of pump-probe spectroscopy. Therefore, streak camera based PL spectroscopy should be conducted in future studies to track longer lifetimes on the order of nanoseconds as reported for dimeric α-crystals [53]. In this study, the dimeric form of the perylene monolayer was formed on the low-temperature substrate; therefore, the observation of a lifetime estimated on the order of nanoseconds is in agreement with that reported for dimeric α-crystals.

Photon emission from ultrathin organic films with a thickness of 2 ML or thicker has been reported for perylene [18] and its derivatives to date [5–8]. The difference from previous studies is that luminescence quenching via nonradiative decay is suppressed on the graphite substrate reported herein, due to the reduced substrate-molecule interaction. More recently, the difference in the efficiency ratio of PL was observed by the systematic variation of the thickness and substrate material [7,8]. It was reported that the exciton relaxation rate is enhanced more on the chemisorbed system than the physisorbed system. Noble metals were used as substrates in these studies [5–8,18], and it is suggested that the strong quenching of excitons across the interface is related to the wave function overlap with that of the metals. In addition, in the case of a perylene derivative monolayer on Ag(111) [8], the presence of an interface state was found to facilitate the transfer of excited carriers at the interface.

In this study, the excimer emission from the perylene 1 ML film was observed because luminescence quenching is suppressed due to the weak substrate-molecule interaction. In addition, no interface state that enhances charge transfer [8] was observed by 2PPE. As reported previously [24], STM images revealed the face to face dimer arrangement with a standing molecular configuration. Decoupled from the substrate, hybridization of the wave functions between the molecule and the substrate is suppressed, which thus opens a decay channel via PL. For perylene α-crystals, the formation of self-trapped excited states by the excimer was reported [12,13] with long lifetimes over several hundreds of picoseconds. Different from free excitons delocalized over the film, self-trapped exciton formation can be mediated by the exciton-phonon coupling, and a similar scheme is suggested for highly luminescent crystals such as pyrene and perylene [9]. In the case of the 1 ML perylene film investigated in this study, the formation of the corresponding self-trapped state might act as a transient state that leads to PL.

IV. CONCLUSIONS

In summary, we have clarified the correlation between the PL properties and excited state dynamics of a perylene monolayer film formed on a graphite surface. The PL properties show temperature-dependent behavior associated with the change in the superstructure. Photon energy dependent 2PPE indicated that the formation of the excited state is responsible for the light emission with visible strength. TR2PPE reveals the formation of the excited state with a lifetime on the order close to nanoseconds. The long lifetime can be understood in the framework of the reduced substrate-molecule interaction; decoupling from the substrate, the excimer does not undergo the ultrafast charge transfer associated with electron/hole scattering to the substrate. The combination of LEED/STM and PL spectroscopy clarified the correlation between the film structure and PL properties, and TR2PPE shows the long lifetime of the excited state that is responsible for visible photon emission at the monolayer limit. We consider that this study provides insight into the excited state carrier dynamics at the interface, which is important for understanding electron transfer and optoelectronics phenomena induced by adsorbed molecules.

ACKNOWLEDGMENTS

T.Y. acknowledges fruitful discussions with Prof. Dr. T. Munakata and Dr. H. S. Kato (Osaka University). This work was supported by the Kakenhi Grants-in-Aid (Grants No. JP16K05656 and No. JP17KT0099), and research funds from the Murata Science Foundation and the Shimadzu Science Foundation.

[1] W. Brütting and C. Adachi, *Physics of Organic Semiconductors*, 2nd ed. (Wiley-VCH Verlag GmbH, Weinheim, 2012).

[2] *Electronic Processes in Organic Electronics*, Springer Series in Materials Science, Vol. 209, edited by H. Ishii, K. Kudo, T. Nakayama, and N. Ueno, (Springer, Berlin, 2015).

[3] Y. Zhang, J. Qiao, S. Gao, F. Hu, D. He, B. Wu, Z. Yang, B. Xu, Y. Li, Y. Shi, W. Ji, P. Wang, X. Wang, M. Xiao, H. Xu, J.-B. Xu, and X. Wang, Probing carrier transport and structure-property relationship of highly ordered organic semiconductors at the two-dimensional limit, Phys. Rev. Lett. **116**, 016602 (2016).

[4] Y. Hasegawa, Y. Yamada, M. Sasaki, T. Hosokai, H. Nakanotani, and C. Adachi, Well-ordered 4CzIPN ((4s,6s)-2,4,5,6-tetra(9-H-carbazol-9-yl)isophthalonitrile) layers: Molecular orientation, electronic structure, and angular distribution of photoluminescence, J. Phys. Chem. Lett. **9**, 863 (2018).

[5] W. Gebauer, A. Langner, M. Schneider, M. Sokolowski, and E. Umbach, Luminescence quenching of ordered π-conjugated molecules near a metal surface: Quaterthiophene and PTCDA on Ag(111), Phys. Rev. B **69**, 155431 (2004).

[6] D. Ino, T. Yamada, and M. Kawai, Luminescence from 3,4,9,10-perylenetetracarboxylic dianhydride on Ag(111) surface excited by tunneling electrons in scanning tunneling microscopy, J. Chem. Phys. **129**, 014701 (2008).

[7] K. Stallberg, A. Namgalies, and U. Höfer, Photoluminescence study of the exciton dynamics at PTCDA/noble-metal interfaces, Phys. Rev. B **99**, 125410 (2019).

[8] K. Stallberg, A. Namgalies, S. Chatterjee, and U. Höfer, Ultrafast exciton dynamics and charge transfer at PTCDA/metal interfaces, J. Phys. Chem. C **126**, 12728 (2022).

[9] H. Nishimura, T. Yamaoka, K. Mizuno, M. Iemura, and A. Matsui, Luminescence of free and self-trapped excitons in α- and β-perylene crystals, J. Phys. Soc. Jpn. **53**, 3999 (1984).

[10] A. Furube, M. Murai, Y. Tamaki, S. Watanabe, and R. Katoh, Effect of aggregation on the excited-state electronic structure of perylene studied by transient absorption spectroscopy, J. Phys. Chem. A **110**, 6465 (2006).

[11] A. Pick, M. Klues, A. Rinn, K. Harms, S. Chatterjee, and G. Witte, Polymorph-selective preparation and structural characterization of perylene single crystals, Cryst. Growth Des. **15**, 5495 (2015).

[12] Y. Ishibashi and T. Asahi, Femtosecond pump–probe microspectroscopy of single perylene nanoparticles, J. Phys. Chem. Lett. **7**, 2951 (2016).

[13] T. Rangel, A. Rinn, S. Sharifzadeh, F. H. Jornada, A. Pick, S. G. Louie, G. Witte, L. Kronik, and J. B. Neaton, Low-lying excited states in crystalline perylene, Proc. Natl. Acad. Sci. USA **115**, 284 (2018).

[14] S. J. Pookpanratana, K. P. Goetz, E. G. Bittle, H. Haneef, L. You, C. A. Hacker, S. W. Robey, O. D. Jurchescu, R. Ovsyannikov, and E. Giangrisostomi, Electronic properties and structure of single crystal perylene, Org. Electronics. **61**, 157 (2018).

[15] M. Botoshansky, F. H. Herbstein, and M. Kapon, Towards a complete description of a polymorphic crystal: The example of perylene, Helv. Chim. Acta **86**, 1113 (2003).

[16] R. E. Cook, B. T. Phelan, R. J. Kamire, M. B. Majewski, R. M. Young, and M. R. Wasielewski, Excimer formation and symmetry-breaking charge transfer in cofacial perylene dimers, J. Phys. Chem. A **121**, 1607 (2017).

[17] W. Ni, G. G. Gurzadyan, J. Zhao, Y. Che, X. Li, and L. Sun, Singlet fission from upper excited electronic states of cofacial perylene dimer, J. Phys. Chem. Lett. **10**, 2428 (2019).

[18] Q. Chen and N. V. Richardson, Optical properties of perylene thin films on Cu(110), J. Phys. Chem. C **114**, 6062 (2010).

[19] B. Lu, H. J. Zhang, Y. S. Tao, H. Huang, H. Y. Li, S. N. Bao, and P. He, Perylene monolayer on the Ru(0001) surface, Appl. Phys. Lett. **86**, 061915 (2005).

[20] K. Manandhar and B. A. Parkinson, Photoemission and STM study of the morphology and barrier heights at the interface between perylene and noble metal (111) surfaces, J. Phys. Chem. C **114**, 15394 (2010).

[21] H. Han, H. J. Zhang, B. Bernhard, Q. Chen, H. Y. Mao, B. Lu, H. Y. Li, P. He, and S. N. Bao, The ordered thin-film growth of organic semiconductor on Ag(110), J. Chem. Phys. **124**, 054716 (2006).

[22] S. Söhnchen, K. Hänel, A. Birkner, G. Witte, and C. Wöll, Molecular beam deposition of perylene on copper: Formation of ordered phases, Chem. Mater. **17**, 5297 (2005).

[23] K. Bobrov, N. Kalashnyk, and L. Guillemot, True perylene epitaxy on Ag(110) driven by site recognition effect, J. Chem. Phys. **142**, 101929 (2015).

[24] T. Yamada, K. Araragi, H. S. Kato, and T. Munakata, Structural characterization and photoluminescence properties of monolayer perylene on graphite surface, J. Phys. Chem. C **124**, 12485 (2020).

[25] See Supplemental Material at http://link.aps.org/supplemental/10.1103/PhysRevB.108.205422 for STM and LEED measurements on 1 ML perylene film at 90 K; photoluminescence spectra of the sample holder; basic concepts of 2PPE excitation processes; assignments of 2PPE spectroscopic features for 1 ML perylene film; logarithmic scale representation of Fig. 3(b1) for 1 ML perylene film; raw TR2PPE spectra for 1 ML perylene film, which includes Refs. [26–31].

[26] P. Tegeder, S. Hagen, F. Leyssner, M. V. Peters, S. Hecht, T. Klamroth, P. Saalfrank, and M. Wolf, Electronic structure of the molecular switch tetra-*tert*-butyl-azobenzene adsorbed on Ag(111), Appl. Phys. A **88**, 465 (2007).

[27] N. Kawakita, T. Yamada, M. Meissner, R. Forker, T. Fritz, and T. Munakata, Metastable phase of lead phthalocyanine films on graphite: Correlation between geometrical and electronic structures, Phys. Rev. B **95**, 045419 (2017).

[28] K. H. Frank, P. Yannoulis, R. Dudde, and E. E. Koch, Unoccupied molecular orbitals of aromatic hydrocarbons adsorbed on Ag(111), J. Chem. Phys. **89**, 7569 (1988).

[29] N. Sai, M. L. Tiago, J. R. Chelikowsky, and F. A. Reboredo, Optical spectra and exchange-correlation effects in molecular crystals, Phys. Rev. B **77**, 161306(R) (2008).

[30] M. Shibuta, K. Yamamoto, K. Miyakubo, T. Yamada, and T. Munakata, Vibrationally resolved two-photon photoemission spectroscopy for lead phthalocyanine film on graphite, Phys. Rev. B **80**, 113310 (2009).

[31] T. Kirchhuebel, S. Kera, T. Munakata, N. Ueno, R. Shiraishi, T. Yamaguchi, K. Yonezawa, T. Ueba, F. Bussolotti, J. Yang, T. Yamada, R. Mori, S. Kunieda, T. Huempfner, M. Gruenewald, R. Forker, and T. Fritz, Role of initial and final states in molecular spectroscopies: Example of tetraphenyldibenzoperiflanthene (DBP) on graphite, J. Phys. Chem. C **124**, 19622 (2020).

[32] T. Yamada and T. Munakata, Spectroscopic and microscopic investigations of organic ultrathin films: Correlation between

geometrical structures and unoccupied electronic states, Prog. Surf. Sci. **93**, 108 (2018).
[33] H. Petek and S. Ogawa, Femtosecond time-resolved two-photon photoemission studies of electron dynamics in metals, Prog. Surf. Sci. **56**, 239 (1997).
[34] X. Y. Zhu, Electronic structure and electron dynamics at molecule–metal interfaces: Implications for molecule-based electronics, Surf. Sci. Rep. **56**, 1 (2004).
[35] J. Güdde and U. Höfer, Femtosecond time-resolved studies of image-potential states at surfaces and interfaces of rare-gas adlayers, Prog. Surf. Sci. **80**, 49 (2005).
[36] P. M. Echenique, R. Berndt, E. V. Chulkov, Th. Fauster, A. Goldmann, and U. Höfer, Decay of electronic excitations at metal surfaces, Surf. Sci. Rep. **52**, 219 (2004).
[37] T. Yamada, N. Ito, N. Kawakita, H. S. Kato, and T. Munakata, Formation and regulation of unoccupied hybridized band with image potential states at perylene/graphite interface, J. Chem. Phys. **151**, 224703 (2019).
[38] T. Yamada, N. Kawakita, C. Okui, and T. Munakata, Hybridization of unoccupied molecular orbital with image potential state at lead phthalocyanine/graphite interface, J. Phys.: Condens. Matter **31**, 044004 (2019).
[39] R. Friedlein, X. Crispin, M. Pickholz, M. Keil, S. Stafström, and W. R. Salaneck, High intercalation levels in lithium perylene stoichiometric compounds, Chem. Phys. Lett. **354**, 389 (2002).
[40] R. Friedlein, Two-photon photoionization by singlet-singlet annihilation in polycrystalline, thin perylene films, Appl. Phys. A **95**, 315 (2009).
[41] H. Auweter, D. Ramer, B. Kunze, and H. C. Wolf, The dynamics of excimer formation in perylene crystals, Chem. Phys. Lett. **85**, 325 (1982).
[42] E. Freydorf, J. Kinder, and M. E. Michel-Beyerle, On low temperature fluorescence of perylene crystals, Chem. Phys. **27**, 199 (1978).
[43] H. Sumi, Two kinds of excimers in α-perylene and pyrene crystals: Origin of Y and V emissions, Chem. Phys. **130**, 433 (1989).
[44] H. Imada, M. Imai-Imada, K. Miwa, H. Yamane, T. Iwasa, Y. Tanaka, N. Toriumi, K. Kimura, N. Yokoshi, A. Muranaka, M. Uchiyama, T. Taketsugu, Y. K. Kato, H. Ishihara, and Y. Kim, Single-molecule laser nanospectroscopy with micro–electron volt energy resolution, Science **373**, 95 (2021).
[45] I. I. Abram, R. A. Auerbach, R. R. Birge, B. E. Kohler, and J. M. Stevenson, Narrow line fluorescence spectra of perylene as a function of excitation wavelength, J. Chem. Phys. **63**, 2473 (1975).
[46] S. Xu, J. Cao, C. C. Miller, D. A. Mantell, R. J. D. Miller, and Y. Gao, Energy dependence of electron lifetime in graphite observed with femtosecond photoemission spectroscopy, Phys. Rev. Lett. **76**, 483 (1996).
[47] K. Ertel, U. Kohl, J. Lehmann, M. Merschdorf, W. Pfeiffer, A. Thon, S. Voll, and G. Gerber, Time-resolved two-photon photoemission spectroscopy of HOPG and Ag nanoparticles on HOPG, Appl. Phys. B **68**, 439 (1999).
[48] M. Shibuta, K. Miyakubo, T. Yamada, and T. Munakata, Angle- and time-resolved two-photon photoemission spectroscopy for unoccupied levels of lead phthalocyanine film, J. Phys. Chem. C **115**, 19269 (2011).
[49] A. Hotzel, Electron dynamics of image potential states in weakly bound adsorbate layers: A short review, Prog. Surf. Sci. **82**, 336 (2007).
[50] T. Ueba, T. Yamada, and T. Munakata, Electronic excitation and relaxation dynamics of the LUMO-derived level in rubrene thin films on graphite, J. Chem. Phys. **145**, 214703 (2016).
[51] R. R. Chance, A. Prock, and R. Silbey, Molecular fluorescence and energy transfer near interfaces, Adv. Chem. Phys. **37**, 1 (1978).
[52] H. S. Kato, Y. Murakami, Y. Kiriyama, R. Saitho, T. Ueba, T. Yamada, and T. Munakata, Decay of the exciton in quaterthiophene-terminated alkanethiolate self-assembled monolayers on Au(111), J. Phys. Chem. C **119**, 7400 (2015).
[53] B. Walker, H. Port, and H. C. Wolf, The two-step excimer formation in perylene crystals, Chem. Phys. **92**, 177 (1985).